A new non-pressure-balanced structure in interplanetary space: Boundary layers of magnetic clouds

Fengsi Wei,[1] Xueshang Feng,[1] Fang Yang,[1] and Dingkun Zhong[1]

Received 16 June 2005; revised 6 November 2005; accepted 16 November 2005; published 10 March 2006.

[1] Here is analyzed the observational data of 70 magnetic cloud boundary layers (BLs) from the Three-Dimensional (3-D) Plasma and Energetic Particle (3DP) and 50 BLs from the Solar Wind Experiment (SWE) instruments on Wind spacecraft from February 1995 to June 2003. From this analysis, we discover that the boundary layer of a magnetic cloud is a new non-pressure-balanced structure different from the jump layer (i.e., shocked front) of an interplanetary shock wave. The main results are that (1) the BL is often a non-pressure-balanced structure with the magnetic pressure decrease associated with the abrupt variation of field direction angle (θ, ϕ) for about 90% and more than 85% of the BLs investigated from 3DP and SWE data, respectively; (2) the events of heated and accelerated plasma in the BLs are about 90%, 85% and 85%, 82% of the BLs investigated, respectively, from 3DP and SWE data; (3) the reversal flows are observed and their occurrence ratio is as high as 80% and 90% of the BLs investigated from 3DP and SWE data, respectively; and (4) the plasma and field characteristics for the BLs are also obviously different from those in the jump layers (JLs) of shock waves. These results show that there exist important dynamic interactions inside the BLs. As a preliminary interpretation, this could be associated with the magnetic reconnection process possibly occurring inside the BLs. Thus the study of the BLs, as a new non-pressure-balanced structure in interplanetary space, could open a ''new window'' for revealing some important physical processes in interplanetary space.

Citation: Wei, F., X. Feng, F. Yang, and D. Zhong (2006), A new non-pressure-balanced structure in interplanetary space: Boundary layers of magnetic clouds, *J. Geophys. Res.*, *111*, A03102, doi:10.1029/2005JA011272.

1. Introduction

[2] Magnetic clouds (MCs), as important interplanetary structures, have been widely investigated [e.g., *Bothmer and Schwenn*, 1994; *Osherovich and Burlaga*, 1997; *Tsurutani and Gonzalez*, 1997; *Farrugia et al.*, 1997] since they were identified in interplanetary space by *Burlaga et al.* [1981]. Many signatures have been used to identify the MC [e.g., *Gosling et al.*, 1987; *Farrugia et al.*, 1994; *Tsurutani and Gonzalez*, 1997; *Lepping et al.*, 1997; *Tsurutani et al.*, 1998]; however, as *Burlaga* [1995] and *Zwickl et al.* [1983] indicated, there is no consistency among those various approaches. Thus the identification and properties of the cloud boundary is an urgent topic to be investigated [*Farrugia et al.*, 1997]. One of the main causes generating such difficulty is that the boundary of the MC is not a simple boundary separating the MC from the solar wind (SW) but a complex boundary layer with internal temporal and spatial structures. In recent years the problem of the boundary layer (BL) draws our attention [*Farrugia et al.*, 1994, 2001; *Bothmer and Schwenn*, 1994; *Tsurutani et al.*, 1988; *Lepping et al.*, 1997; *Wei et al.*, 2003a, 2003b]. The BL concept and identifying criteria have been suggested by *Wei et al.* [2003a]. The BL could be characterized by the magnetic signatures (the intensity drop and the abrupt azimuthal changes, $\Delta\phi \sim 180°$, and latitudinal changes, $\Delta\theta \sim 90°$, in the magnetic field) and the corresponding plasma's ''three-high state'' (relatively high proton temperature, high proton density, and high plasma beta) and the following ''three-low state'' (relatively low proton temperature, low proton density, and low plasma β) that separates the magnetic cloud body from the boundary layers (however, the density is a very unreliable parameter to use in any aspect of MC identification). It implies that the MC's BL is affected by certain dynamic interactions between the MC and the SW and is not a simple ''transition layer.'' Analysis of magnetic structure of the BLs shows that the cloud's BL possesses a magnetic structure different from that in the SW and the MC in many aspects, such as the fluctuations of interplanetary magnetic fields, ''walks'' of the tips of the field vectors in the maximum variance plane composed of the maximum and medium variance directions or distributions of the ϕ, θ angles in the BL [*Wei et al.*, 2003b]. Here, we will further analyze the plasma characteristics inside the

[1]SIGMA Weather Group, Key Laboratory for Space Weather, Center for Space Science and Applied Research, Chinese Academy of Sciences, Beijing, China.

0148-0227/06/2005JA011272$09.00

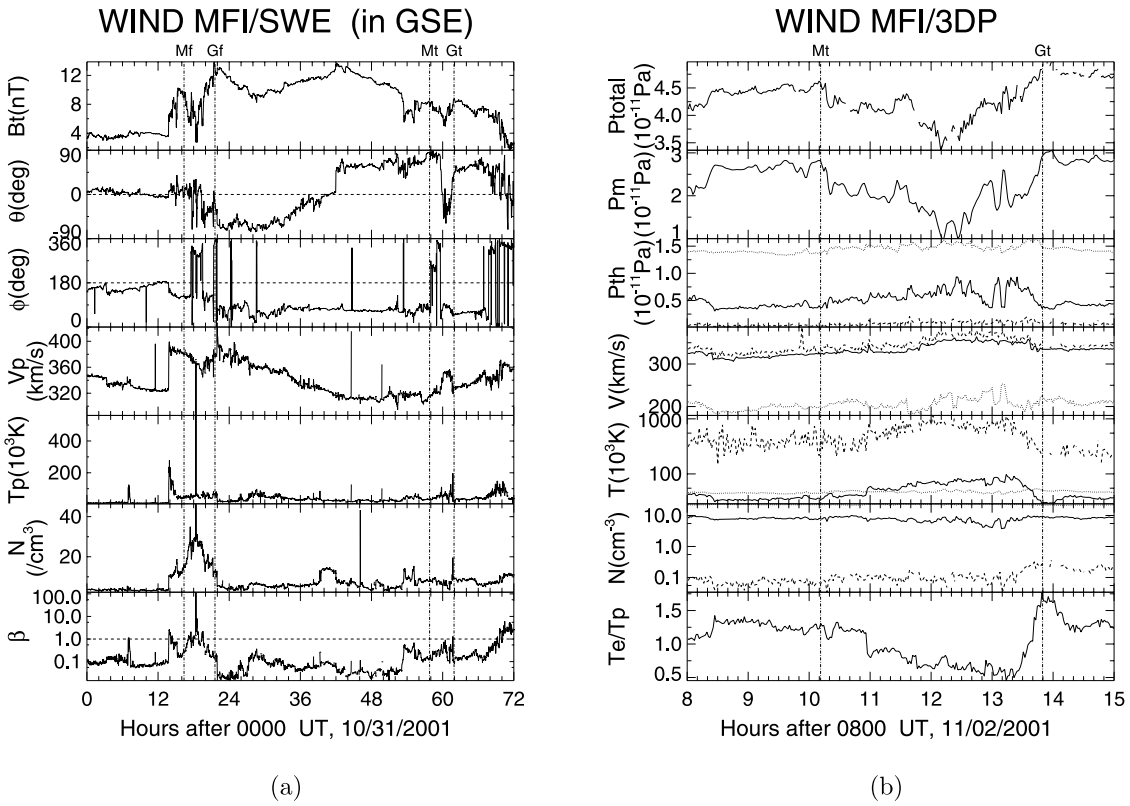

Figure 1. (a) Observation of a magnetic cloud on 31 October 2001, where M_f, G_f and M_t, G_t indicate the boundaries of the front and tail BLs, respectively; and (b) its non-pressure-balanced structure from the tail BL, $M_t - G_t$, where the total pressure (P_T), magnetic pressure (P_m), thermal pressure (P_{th}), velocity (V), temperature (T), number density (N) and temperature ratio (T_e/T_p) between electron and proton are given from the top to the bottom. In the figure the solid, dotted, and dashed lines represent the proton, electron, and α particle, respectively.

cloud BL to enhance a basic understanding of the interactions occurring between the MC and the SW. The results presented in this paper show that the BL is a new non-pressure-balanced structure different from the JL in the behavior of magnetic pressure, temperature, density, particle acceleration, heating, field's directional angle variation, reversal plasma flow, and magnetic field intensity. It is clear that the study of dynamic manifestations and possible formation mechanism occurring in the BLs will be very interesting. We expect that the study of the BLs would provide a "new window" to reveal some of the significant physical processes occurring in interplanetary space.

2. Observational Data

[3] Using the data provided by Wind spacecraft, we analyze the plasma characteristics of 70 cloud BLs from Three-Dimensional (3-D) Plasma and Energetic Particle (3DP) (February 1995–June 2003) and 50 cloud BLs from the Solar Wind Experiment (SWE) (February 1995–May 2001), some BLs appear in both sets of data. They are selected based on the MCs provided by Lepping et al. (http://lepmfi.gsfc.nasa.gov/mfi/mag_cloud_pub1.html) and the BL concept and identification criteria [*Wei et al.*, 2003b]. Here, it should be noticed that the valid electron data of the SWE on Wind are available from February 1995 to May 2001 only, where the electron temperatures are calculated from the second moment of the velocity distribution. The "moment temperature" is generally higher than the "core temperature" calculated by fitting a Maxwellian distribution to the main part of the velocity distribution [*Burlaga*, 1995]. The "core temperature" is available from 3DP on Wind in the period of February 1995–2003. The proton data of 3DP is nearly the same as that of SWE. Now we compare the plasma characteristics from the 3DP data with the SWE data. As an example from 3DP on WIND, a MC event is given in Figure 1a. The cloud begins at ≈2118 UT on 31 October 2001 and ends at ≈1018 UT on 2 November 2001. It drove a shock wave with the shock front at ≈1400 UT on 31 October 2001. The cloud's front and tail BLs are indicated by the lines labeled by M_f, G_f and M_t, G_t, respectively. The basic characteristics for these BLs are that a dip in the magnetic field strength is associated with an abrupt change in the field direction angles ϕ and θ ($\Delta\theta \approx 90°$, $\Delta\phi \approx 180°$) and an increase in the temperature, T_p, number density, N_p, and plasma β as indicated by *Wei et al.* [2003a]. Figure 1b gives the total pressure, P_T, magnetic pressure, P_m, thermal pressure, P_{th}, and parameters T, N, and T_e/T_p inside the tail BL, $M_t - G_t$, the ambient MC and SW, where the solid, dotted, and dashed lines represent the proton, electron, and α particles, respectively. As another example taken from SWE on Wind, the basic plasma

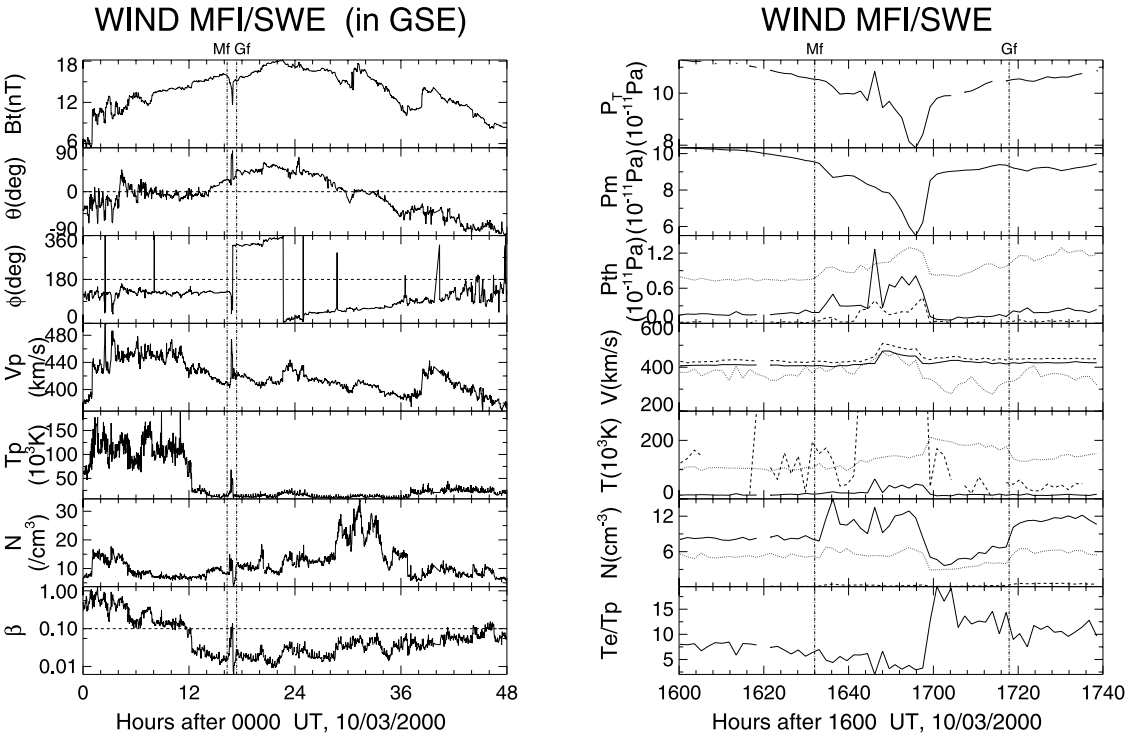

(a) (b)

Figure 2. (a) Observation of a magnetic cloud on 3 October 2000 from Wind, in which M_f, G_f indicate the position of the BL; and (b) the pressure and the plasma parameters in the BL. The meanings of all the symbols are the same as those in Figure 1. Here only α particles are taken from 3DP data.

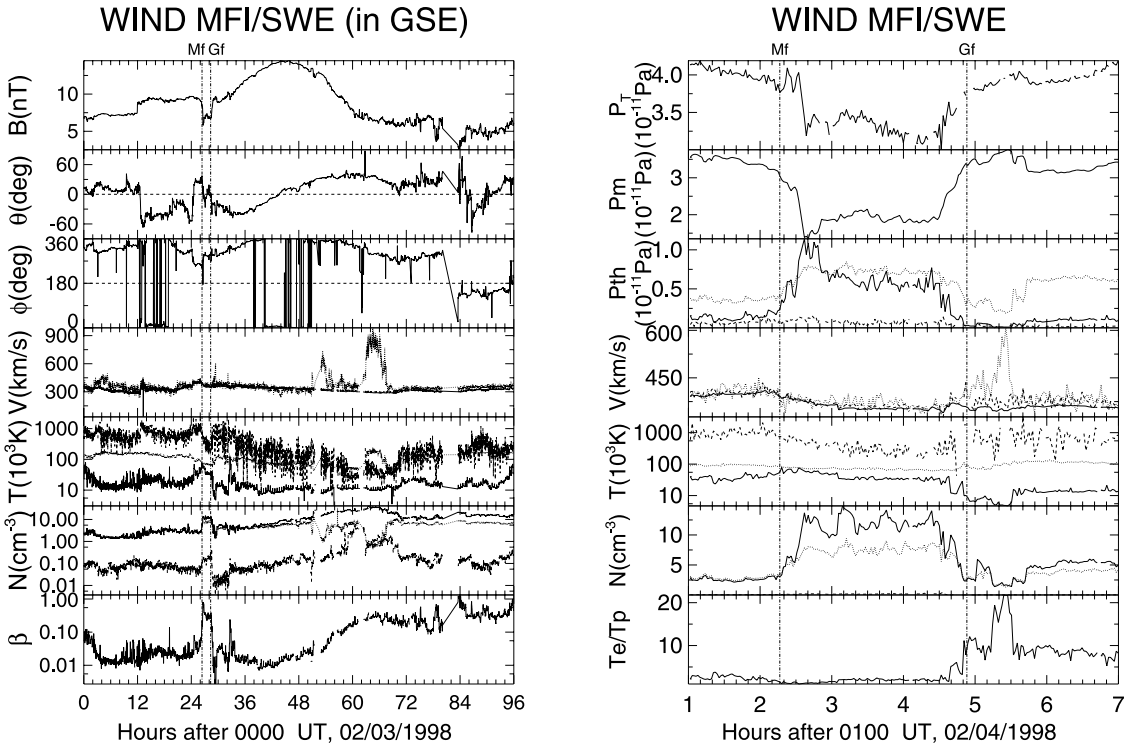

(a) (b)

Figure 3. (a) An example of the total pressure, $P_{T,BL}$, decrease in the BL of a magnetic cloud observed by Wind on 4 February 1998, and (b) the pressures and plasma parameters (see Figure 1b) in the BL ($M_f - G_f$), in which only α particles are taken from 3DP data.

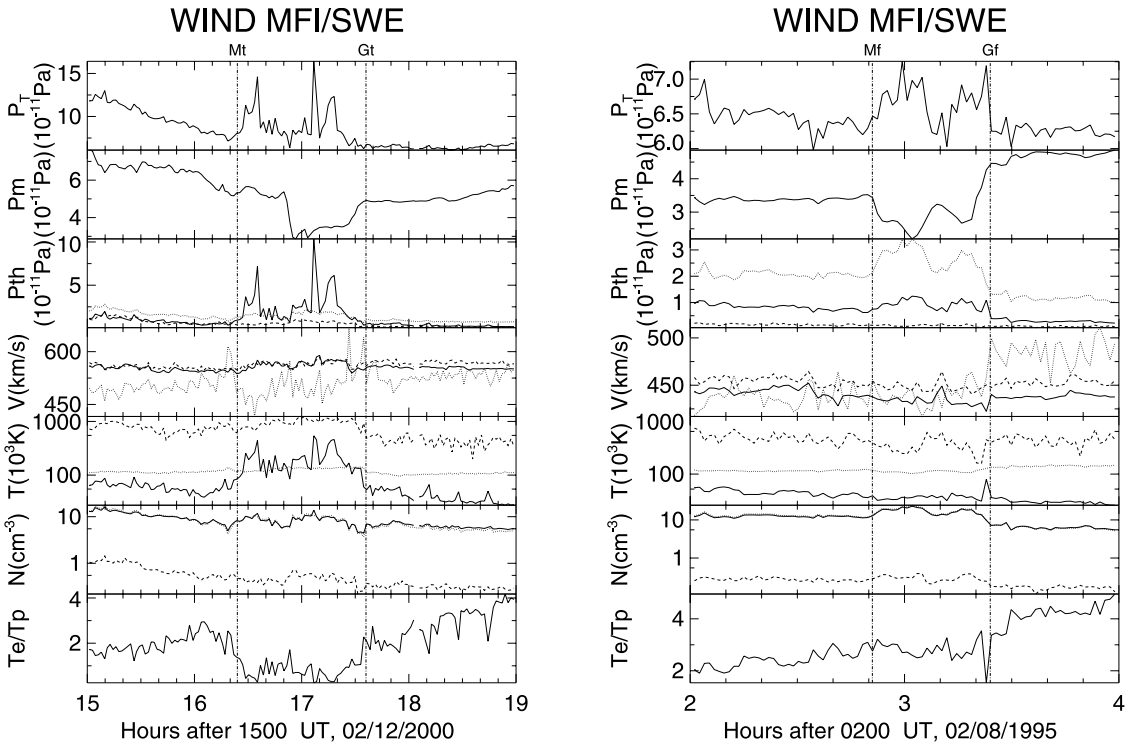

Figure 4. Two examples for the total pressure, $P_{T,BL}$, increase in the BLs, (a) 1618–1733 UT, and (b) 0250–0326 UT, which are associated with two magnetic clouds beginning at ≈1733 UT on 12 February 2000 and at ≈0326 UT on 8 February 1995, respectively. The related changes of the various pressures (P_t, P_m, P_{th}) and the plasma parameters (V, T, N, and T_e/T_p) in the BLs are given in Figures 4a and 4b, respectively. Here the α particles are taken from 3DP data.

characteristics of a MC and its BL are given in Figures 2a and 2b, respectively. The MC event shown in Figure 2a begins at ≈1703 UT on 3 October 2000 and ends at ≈1406 UT on 4 October 2000. It drove a shock wave with the shock front at ≈0100 UT on 3 October 2000. The main features of the shocked sheath region are the abrupt jumps in the basic parameters, such as magnetic field, speed, temperature, and density. A boundary layer, denoted by the two lines labeled by M_f and G_f, is located in 1633–1703 UT and its basic characteristics as we see in Figure 1 are discovered again for this example. Figure 2b gives the total pressure P_T, magnetic pressure P_m, thermal pressure P_{th}, and parameters V, T, N, and T_e/T_p inside the BL. The difference of the electron data from 3DP and SWE mainly lies in the magnitude of the temperature, density, and velocity. The results from SWE are frequently larger than those from 3DP.

[4] From Figures 1b and 2b we can see that the BLs are a non-pressure-balanced structure where the acceleration and heat are also observed. Hence we speculate that these plasma characteristics inside the BLs could be caused by certain dynamic processes occurring in the BLs. Further analysis will be given in section 3. Here, it should be mentioned that the contribution of α particles to the thermal pressure has also been included in the analysis. Although the higher ratio of α - temperature, T_α/T_p, on the average, is ≈3 near 1 AU [*Marsch et al.*, 1982], the low abundance, N_α/N_p is generally ≲3% near 1 AU [*Steinberg et al.*, 1996] such that the contribution of α particles pressure relative to the proton pressure, $P_{T,\alpha}/P_{T,p}$, is ≈2∼10% only. Hence α particles play no important role in the total pressure, $P_{T,L}$, inside the BLs, as seen in Figures 1–8. Below, we will report some results analyzing plasma characteristics of the 70 BLs from 3DP in February 1995–June 2003 and the 50 BLs from SWE in February 1995–May 2001.

3. Analyses and Results

3.1. A Non-Pressure-Balanced Structure

[5] With regard to the total pressure variations across interplanetary structures, there exist some pressure-balanced and non-pressure-balanced structures. Tangential and rotational discontinuities and sector boundaries are typical examples of pressure-balanced structures [*Burlaga*, 1968, 1971; *Burlaga et al.*, 1990; *Belcher and Davis*, 1971]. Magnetic holes are commonly pressure balanced structures [*Burlaga et al.*, 1990]. Although ''D-Sheets'' greatly resemble this kind of the BL, their differences would be obvious in the definition, plasma features, occurrence rate, and timescale, etc. [*Burlaga*, 1968; *Turner et al.*, 1977; *Fitzenreiter and Burlaga*, 1978; *Winterhalter et al.*, 1994; *Wei et al.*, 2003a]. Also, the JL of an interplanetary shock wave is an example of a non-pressure-balanced structure

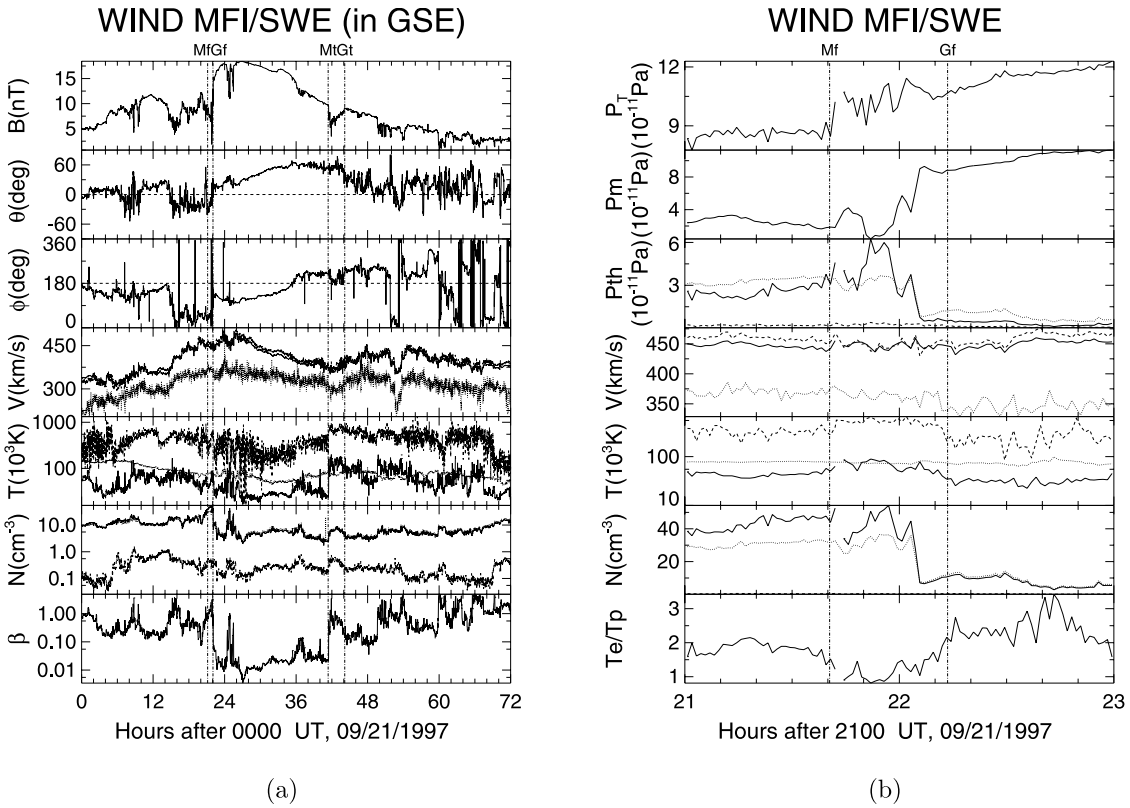

Figure 5. (a) Observational example for the case, $P_{T,SW} < P_{T,BL} < P_{T,MC}$, in the BL ($M_f - G_f$) of a magnetic cloud on 21 September 1997 and (b) the pressures and plasma parameters in the BL (2140–2208 UT), in which the α particles are taken from 3DP data.

with the magnetic pressure increase usually not associated with significant changes in field direction, where significant dynamic interactions are well known [*Burlaga*, 1995]. Which kind of structure does the BL belong to? Obviously, the property of dynamic interaction between the MC and the SW is an interesting topic.

[6] We know that the solar wind's total pressure, $P_T = P_m + P_{th}$, with the thermal pressure, $P_{th} = N_p kT_p + N_e kT_e + N_\alpha kT_\alpha$, $N_\alpha kT_\alpha$, and the magnetic pressure, $P_m = B^2/8\pi$, where the subscripts p, e, and α stand for the proton, electron, and α particles, respectively. The pressure-balanced structures are structures across which the total pressure is constant [*Burlaga*, 1995]. By analyzing the 70 BLs from 3DP and the 50 BLs from SWE, we find that the BL is a non-pressure-balanced structure across which the total pressure is not a constant in both 3DP and SWE data. Several basic cases in the total pressure, P_T, can be seen from the following cases.

3.1.1. Case 1: $P_{T,BL} < P_{T,SW}$, $P_{T,MC}$

[7] An example is given in Figure 3a, which is a MC beginning at ≈0217 UT on 4 February 1998 with its front BL shown by the two vertical lines M_f and G_f. Figure 3b shows various pressure changes in the BL in Figure 3a. We can see that a dip of the magnetic pressure in the BL, $P_{m,BL}$, is not compensated by the increase of the thermal pressure, $P_{th,BL}$. This feature can be observed in 80% of the BLs from 3DP and in 27.8% of the BLs from SWE, respectively. The latter has a lower percentage because the temperature in 3DP is lower than that in SWE. In the BLs satisfying this condition, $P_{T,BL} < P_{T,SW}$, $P_{T,MC}$, the level of the averaged fluctuations in the $P_{T,BL}$ is ≲10% of the maximum variation, $\Delta P_{T,BL}$, inside the BL.

3.1.2. Case 2: $P_{T,BL} > P_{T,SW}$, $P_{T,MC}$

[8] The total pressure increases inside the BL observed by Wind. Figure 4a gives the variations of P_{th}, P_m, and P_T in the tail BL (1618–1733 UT) of a MC beginning at ≈1733 UT on 12 February 2000, where the main contribution to the $P_{T,BL}$ comes from the heating of the protons in the BL. Another example is given in Figure 4b, where the total pressure increases inside the front BL (0250–0326 UT) of a MC beginning at ≈0326 UT on 8 February 1995 was observed by Wind. The higher electron thermal pressure occupies a significant portion of the total pressure in the BL. The BLs categorized in Case 2 are observed only by SWE and occupies about 14.8% of 50 BLs investigated, where the averaged fluctuation level in the $P_{T,BL}$ is about 11.0% of the maximum variation, ΔP_T, in the BL. However, no BL of this case was observed by 3DP. Since the core temperature from 3DP is often lower than the moment temperature from SWE, the increase in the $P_{th,BL}$ should be lower than the decrease in $P_{m,BL}$ so that the $P_{T,BL}$ is often lower than $P_{T,SW}$ and $P_{T,MC}$, as seen in Case 1.

3.1.3. Case 3: $P_{T,SW} < P_{T,BL} < P_{T,MC}$ or $P_{T,SW} > P_{T,BL} > P_{T,MC}$

[9] An example for this kind of MC is given in Figure 5a, where the MC begins at ≈2208 UT on 21 September 1997 and its front BL (2146∼2200 UT) is labeled by M_f and G_f. The changes of the various pressures in the BL are given in

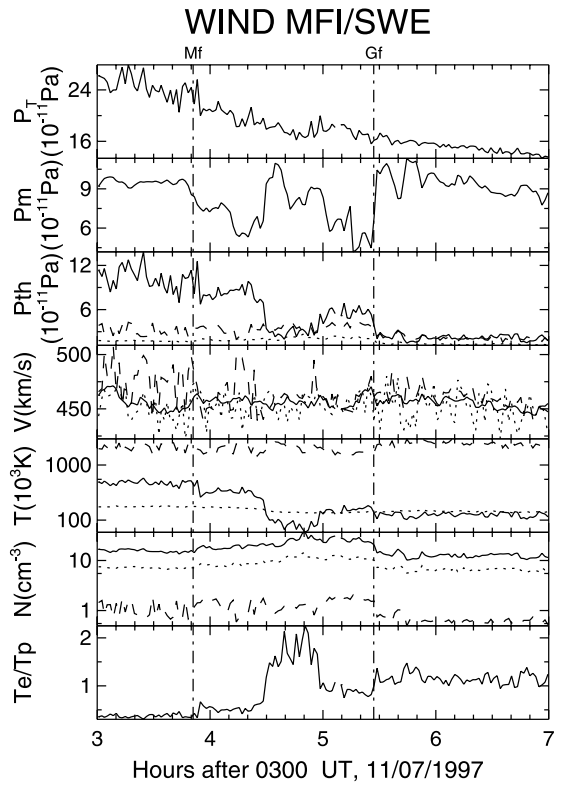

Figure 6. An example for the case, $P_{T,SW} > P_{T,BL} > P_{T,MC}$, in the BL (0352–0528 UT) of a magnetic cloud beginning at ≈0530 UT on 7 November 1997. The variations of the basic parameters in the SW, the BL and the MC are given here, in which the α particles are taken from 3DP data.

Figure 5b. The feature, $P_{T,SW} < P_{T,BL}$, is mainly caused by the thermal pressure increase being larger than the dip in the magnetic pressure in the BL, and the feature, $P_{T,BL} < P_{T,MC}$, is mainly determined by higher magnetic pressure in the MC. Another observational example of a BL (0352–0528 UT) of a cloud is on 7 November 1997, shown in Figure 6, where the thermal pressure in the ambient solar wind, $P_{T,SW}$, is much bigger than that in the MC, and $P_{T,BL}$, is intermediate. Note that the minimum thermal pressure is in the MC. This case occupies about 20% of the BLs of 3DP and 51.9% of SWE, respectively. The statistical fluctuation level in $P_{T,BL}$ is ≈12% of the maximum variation, ΔP_T, inside the BL.

3.1.4. Case 4: $P_{T,SW} \approx P_{T,BL} \approx P_{T,MC}$

[10] This type of BL is also observed in the cloud's BLs as shown in Figure 7, where the variation in the thermal pressure of electron and proton in the BL (0820–0940 UT) of a MC on 1 July 2000, is largely balanced by the variations in the magnetic pressure in the ±6% range of the P_T. However, it was seldom observed, occurring in about 5.6% in the BLs from SWE and almost not observed in the BLs from 3DP.

[11] The statistical results of the basic plasma parameters in the SW, BL, and MC, from 3DP data, are given in Tables 1a, 1b, and 1c. From Table 1a we can see that the percentage of the events with increasing temperature and density in the BLs, compared with adjacent SW and MC, is as high as 96% for the case $T_p * T_e$ (i.e., including T_p and/or T_e) and 86% for the case $N_p * N_e$ (i.e., including N_p and/or N_e), respectively, so that the events satisfying $P_{th,BL} > P_{th,SW}$, $P_{th,MC}$ occupy a high fraction 84% of cases. Since the BL is generally a magnetic pressure decrease structure, the dip in the $P_{m,BL}$ could not be compensated by the increase of $P_{th,BL}$ in BLs for 80% of the BLs investigated. This corresponds to high plasma β property of 80% BLs (see Table 1b). In addition, the events with $P_{T,SW} > P_{T,BL} > P_{T,MC}$ or $P_{T,SW} < P_{T,BL} < P_{T,MC}$ satisfy about 20% of the investigated BLs. It is evident that there are almost no BLs across which the P_T is a constant, i.e., $P_{T,SW} \neq P_{T,BL} \neq P_{T,MC}$ for almost all BLs investigated. Table 2 gives the statistical results from SWE data for the plasma characteristics inside the BLs. From Tables 2a and 2b we can see that the event rate of the temperature increase is as high as 81% for T_p and/or T_e and 78.2% for N_p and/or N_e so that the case $P_{T,SW} \neq P_{T,BL} \neq P_{T,MC}$ is as high as 94.4%. This result from SWE data is basically consistent with Tables 1a, 1b and 1c from 3DP data. Combining Tables 1a, 1b and 1c (from 3DP data) and Table 2 (from SWE data), the statistic results show that the BLs are a non-pressure-balanced structures. Their statistical error, on average, is about ≲10% in both 3DP and SWE.

[12] Why is the BL a non-pressure-balanced structure? What are the related dynamic manifestations and the possible physical process? These questions urge us to analyze the dynamic manifestations in the BLs below.

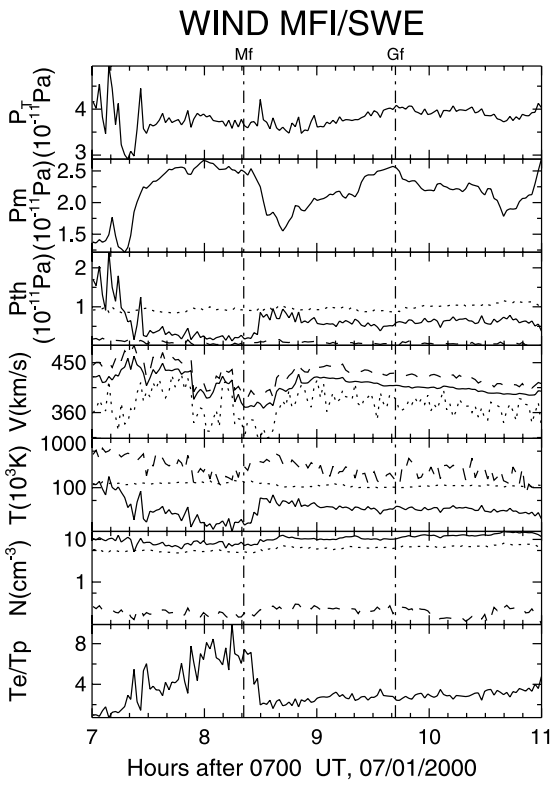

Figure 7. Observational case, $P_{T,SW} \approx P_{T,BL} \approx P_{T,MC}$, in a front BL ($M_f - G_f$) of a magnetic cloud beginning at ≈0940 UT on 1 July 2000, where the variations of the basic parameters are given in the SW, the BL, and the MC, respectively. Here the α particles are taken from 3DP data.

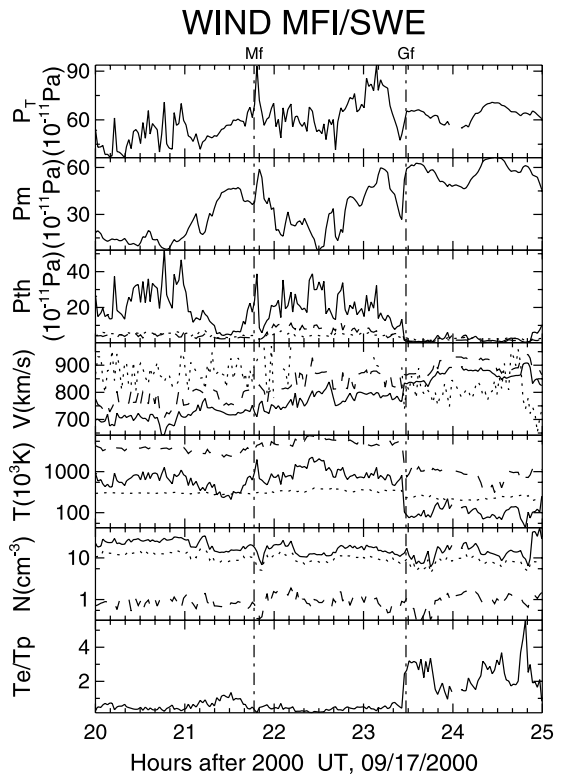

Figure 8. An example of the acceleration and heating for the protons, electrons, and α particles in the BL (2146–2329 UT) of a magnetic cloud beginning at ≈2329 UT on 17 September 2000, in which the velocity of electrons (>1000 km/s) accelerated in the BL exceeds the scale range given in the velocity figure and only α particles are taken from 3DP data.

3.2. Accelerating and Heating of Protons and Electrons

[13] The non-pressure-balanced structures are often associated with certain important dynamic interactions. For example, the JL is a non-pressure-balanced structure across which the total pressure abruptly rises. This pressure increase is associated with dynamical behavior, i.e, the heating, accelerating, and compressing of the plasma, and the compressed magnetic field (see discussions in section 4). Heating and accelerating have also been observed in the BLs, although their behaviors are different from those in the JLs of shock waves. As already observed in Figure 2b, the increased values of velocity and temperature relative to the SW reach ~55 km/s, ~110 km/s, and ~100 km/s and ~5.0×10^4 K, ~1.0×10^5 K, and ~2.6×10^5 K for the protons, electrons, and α particles, respectively. Figure 8 shows another typical example of acceleration and heating for protons, electrons, and α particles in the BL (2146–2329 UT) of a MC beginning at ≈2330 UT on 17 September 2000. The temperature increase, from the two sides, M_f and G_f, to the center of the BL, reaches a factor of ≈4.0, from 4.0×10^5 K to 16.0×10^5 K, ≈1.3 (from 3×10^5 to 4.0×10^5 K) and 2.5 (from 3.0×10^6 to 7.5×10^6 K), for the proton, electron, and α particle, respectively, and similarly, the velocity increase, ΔV, is about 110 km/s, 120 km/s, and 150 km/s for these particles, respectively. Sometimes, the acceleration and/or heating occur only in one or two components of protons, electrons, and α particles.

[14] Table 1a gives a statistic result for velocity variations of the protons and electrons in the BLs from 3Dp data. The events with accelerated V_p and V_e in the BLs reach 46% and 74% in the 70 BLs, respectively. When we do not distinguish the protons from electrons, as noted by the asterisk symbol in Table 1a, these accelerated events, $V_p * V_e$, occupy a large fraction of 85% of the BLs investigated. The events of heated protons and/or electrons, $T_p * T_e$, as deduced from Table 1a, is as high as 96%. Similarly, from Table 2a we can see that the events without distinguishing accelerated protons from electrons, $V_p * V_e$, occupy a large fraction of 74.5% in the investigated 50 BLs, and the heated events $T_p * T_e$, are as high as 81%. It is clear that the acceleration and heating of the plasma in the BL is a common phenomenon. However, this property is not observed in the adjacent SW and MC. It can be believed that the energy used for accelerating plasma would be related with the same process through which the protons and electrons are heated. One of the candidate processes is magnetic reconnection, possibly generated in the BLs. As a rough estimation, from the point of view of energetics, the magnetic energy from the magnetic annihilation (Figure 1a) is about 5.4×10^{-11} J, which could provide the needed energy for raising the plasma thermal energy (≈1.2×10^{-11} J)

Table 1a. Statistic Results of the 70 BLs from 3DP on Wind of the Plasma Parameters T_p, T_e, $T_p * T_e$, N_p, N_e, $N_p * N_e$, V_p, V_e, and $V_p * V_e$[a]

	Increase, %	Approximate, %	Decrease, %
T_p	88	9	4
T_e	64	29	8
$T_p * T_e$	96	3	1
N_p	84	11	7
N_e	44	44	12
$N_p * N_e$	86	9	5
V_p	46	53	1
V_e	74	22	4
$V_p * V_e$	85	15	0

[a]Here the asterisk represents protons and/or electrons (i.e., without distinguishing protons from electron in statistic results.

Table 1b. Statistic Results of the 70 BLs from 3DP on Wind With the Thermal Pressure, P_{th}, Total Pressure, P_T, and Plasma Parameter, β[a]

	BL > SW, MC, %	BL < SW, MC, %	SW > BL > MC or SW < BL < MC, %	SW ~ BL ~ MC, %
P_{th}	84	0	16	0
P_T	0	80	20	0
β	80	0	20	0

[a]Here the letters SW, BL, and MC represent the solar wind, boundary layers, and magnetic cloud.

Table 1c. Statistic Results of the 70 BLs from 3DP on Wind With the Reversal Flows in V_x, V_y, and V_z

	Reversal in V_x, V_y, V_z, %
Reversal in one	19
Reversal in two	40
Reversal on all	24
No reversal	17

Table 2a. Statistic Results of the 50 BLs from SWE on Wind of the Plasma Parameters T_p, T_e, $T_p * T_e$, N_p, N_e, $N_p * N_e$, V_p, V_e, and $V_p * V_e$[a]

	Increase, %	Approximate, %	Decrease, %
T_p	78.9	13.5	7.6
T_e	34.0	60.4	5.7
$T_p * T_e$	81.0	12.7	5.5
T_α	71.0	13.3	15.6
N_p	78.2	10.9	10.9
N_e	72.7	12.7	14.5
$N_p * N_e$	78.2	10.9	10.9
V_p	50.9	34.5	14.5
V_e	64.8	16.7	18.5
$V_p * V_e$	74.5	10.9	14.5
V_α	50.0	26.1	23.9

[a]Here the asterisk represents protons and/or electrons (i.e., without distinguishing protons from electron in statistic results.

and the kinetic energy ($\approx 3.0 \times 10^{-11}$J). In what follows, the problem concerning magnetic reconnection will be further analyzed based on the characteristics of reversal flows and magnetic field in the BLs.

3.3. Reversal Flow

[15] The reversal plasma flow (or jet) is also an important indicator for understanding dynamic interactions. For example, the reversal flow near an X-neutral line is regarded as a basic feature of magnetic reconnection occurring in the solar atmosphere, the Earth's magnetopause, and magnetotail [*Paschmann et al.*, 1979; *Innes et al.*, 1997; *Øieroset et al.*, 2001]. On the basis of the data from 3DP and MFI on Wind, we analyze the plasma flows from 70 BLs and find that the reversal flows often exist in the BLs investigated. As an example, Figure 9a displays a typical MC recorded by Wind spacecraft on 9 August 1999, whose front and tail boundary layers are labeled by $M_f - G_f$ and $M_t - G_t$, respectively. A complex reversal flows in the tail BL, $M_t - G_t$, are shown in the regions $D_1 - D_2$ and $D_3 - G_t$ in Figure 9b, as denoted by the oblique dotted line. The flow reversal from +20 km/s to −20 km/s in V_y and from +10 km/s to −10 km/s in V_z, is seen in the region $D_3 - G_t$ in Figure 9b, respectively, and that in V_x, superposed on the background solar wind, is from +15 km/s to −15 km/s. If we adopt the plus and minus signs to stand for "positive" and "negative" and the subscript 1, 2 denote the "entrance side" and "outgoing side," respectively, we can successfully see the reversal flows and fields in the region $D_1 - D_2$: $+V_x1 \rightarrow -V_x2$, $-B_x1 \rightarrow +B_x2$, $+V_y1 \rightarrow -V_y2$, $-B_y1 \rightarrow +B_y2$, $+V_z1 \rightarrow -V_z2 + B_z1 \rightarrow -B_z2$ and in the region $D_3 - G_t$: $+V_x1 \rightarrow -V_x2$, $+B_x1 \rightarrow -B_x2$, $+V_y1 \rightarrow -V_y2$, $+B_y1 \rightarrow -B_y2$, $-V_z1 \rightarrow +V_z2$, $-B_z1 \rightarrow +B_z2$. The reversal change in the magnetic field polarity is also clear here. Figure 10a gives another typical magnetic cloud recorded by Wind spacecraft in 1036–1900 UT on 2 June 1998, where M_f, G_f and M_t, G_t, respectively, show the front and tail BLs of the cloud. According to the cloud's central velocity, 410 km/s ($\theta = 0°$), the cloud was expanding at a speed ≈20 km/s, about half the local Alfvenic velocity V_A(≈36 km/s), relative to the background solar wind (390 km/s). Simultaneously, it was overtaken by a high-speed stream beginning at ≈2000 UT. Therefore the stronger interactions occur in both the front and tail boundary layers of the cloud, which can be seen more clearly from the evident variations of the basic parameters in the BL. Here, let us look at the complex tail BL. The reversal flows in the tail BL, $M_t - G_t$, appear in the regions $M_t - D_1$ and $D_3 - D_4$ denoted by the oblique dotted line in Figure 10b, where the parameters B_t, θ, ϕ, B_x, B_y,B_z, and V_x, V_y, V_z are also given. The reversal flows in V_y, V_z, and V_x are very clear in the interval $M_t - D_1$, the maximum changes run from −10 km/s to +40 km/s in the V_y and from −20 km/s to +20 km/s in both V_z and V_x. The reversal flows is also clearly observed in the interval $D_3 - D_4$ and its velocity changes from +20 km/s, −15 km/s to −15 km/s, +30 km/s in V_x and V_z, respectively. In addition, the variations in the field polarities are also found in the BL.

[16] The statistical results for the reversal flows are given in Table 1c from 3DP data and Table 2c from SWE data, where the events of reversal flows existing in one, two, and three components of velocity (V_x, V_y, V_z) are 19%, 40%, 24% and 14%, 44%, 30% of the investigated BLs in Table 1c and 2c, respectively. The events with the reversal flows, whether observed in one, two, or three components of velocity, then occupy 83% in the 70 BLs from 3DP data and 88% in 50 BLs from SWE data, respectively. The events with the reversal fields occupy almost the same rate as those with the reversal flows in the BLs investigated (omitted in Table 2b). Thus the reversal flows exist generally and are accompanied by the reversal fields in the BLs. However, such cases are not often observed in the SW or in the MC. These reversal flows have a common feature, i.e., they are associated with the dips in the magnetic field intensity, the obvious changes in the field directions, as well as the reversal fields in B_x, B_y, and B_z, which are especially evident in Figure 9b. Generally, these features may be observed in the magnetic reconnection region only, as observed in the magnetic reconnection region of the Earth's magnetotail [*Øieroset et al.*, 2001].

Table 2b. Statistic Results of the 70 BLs from 3DP on Wind With the Thermal Pressure, P_{th}, Total Pressure, P_T, and Plasma Parameter, β[a]

	BL > SW, MC, %	BL < SW, MC, %	SW > BL > MC or SW < BL < MC, %	SW ∼ BL ∼ MC, %
P_{th}	18.5	81.5	0	0
P_T	51.9	14.8	27.8	5.6

[a]Here the letters SW, BL, and MC represent the solar wind, boundary layers, and magnetic cloud.

Table 2c. Statistic Results of the 70 BLs from 3DP on Wind With the Reversal Flows in V_x, V_y, and V_z

	Reversal in V_x, V_y, V_z, %
Reversal in one	14
Reversal in two	44
Reversal on all	30
No reversal	12

4. Discussions and Conclusions

[17] In order to understand the plasma characteristics occurring inside the BLs reported here, we give a possible physical interpretation. It is known that the heating, reversal flows, reversal fields, and field strength dip associated with the abrupt field direction variations ($\Delta\phi \approx 180°$, $\Delta\theta \approx 90°$)

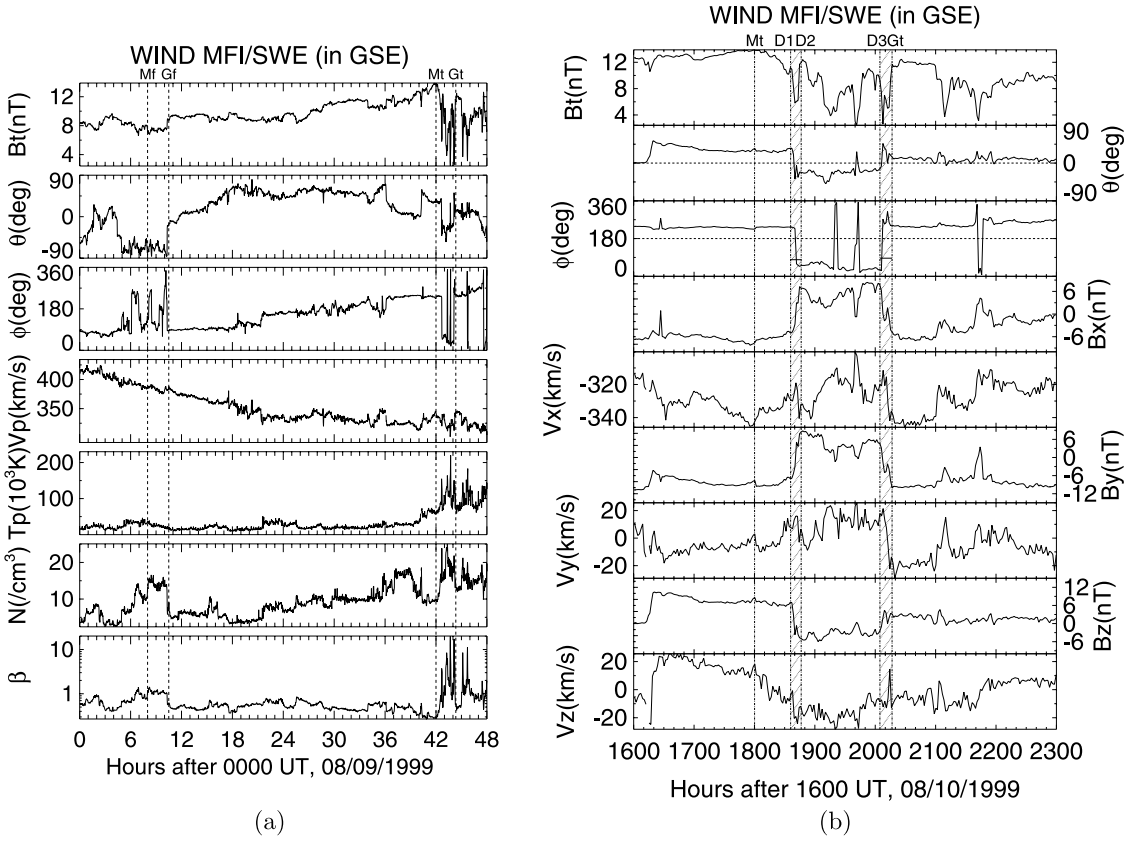

Figure 9. (a) An example for the reversal plasma flows and fields from the BL ($M_t - G_t$) of a MC observed by Wind on 9 August 1999, and (b) B_t, θ, ϕ, B_x, V_x, B_y, V_y, B_z and V_z in the regions $D_1 - D_2$ and $D_3 - G_t$ of the BL ($M_t - G_t$). Here, $D_2 - D_3$ is the transit region.

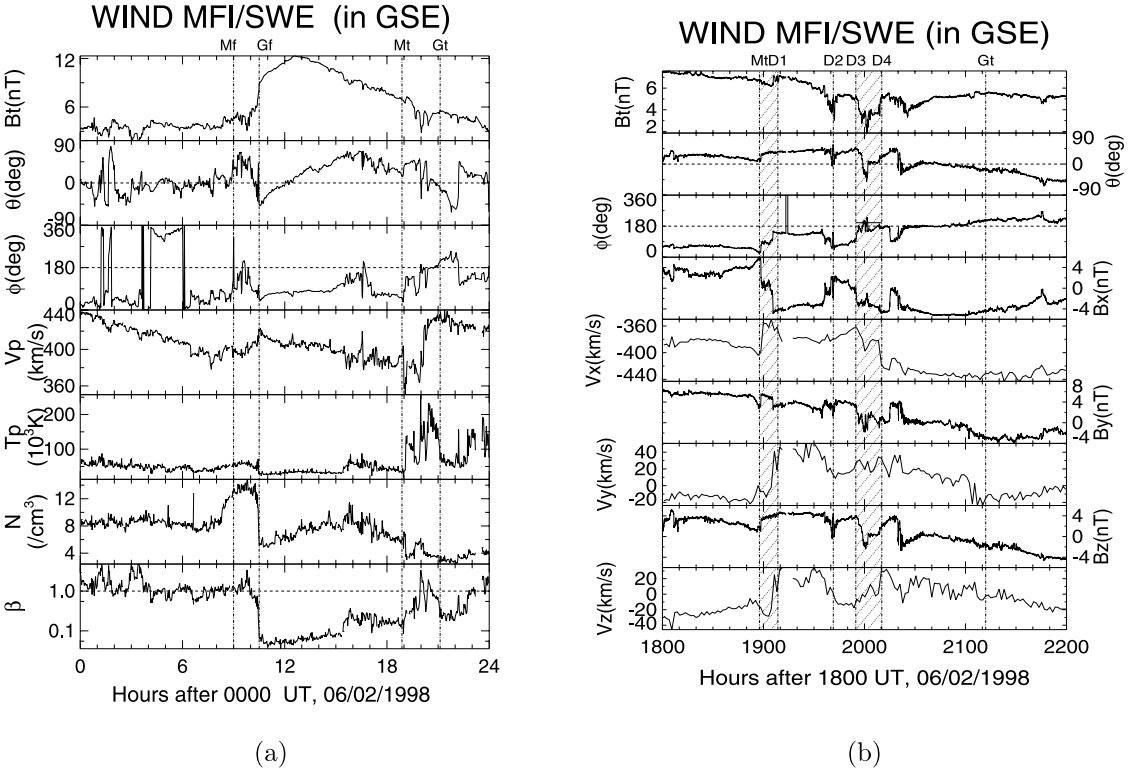

Figure 10. (a) Observation of a MC on 2 June 1998, and (b) the reversal flows and fields in the BL ($M_t - G_t$) are given in those regions denoted by oblique short lines.

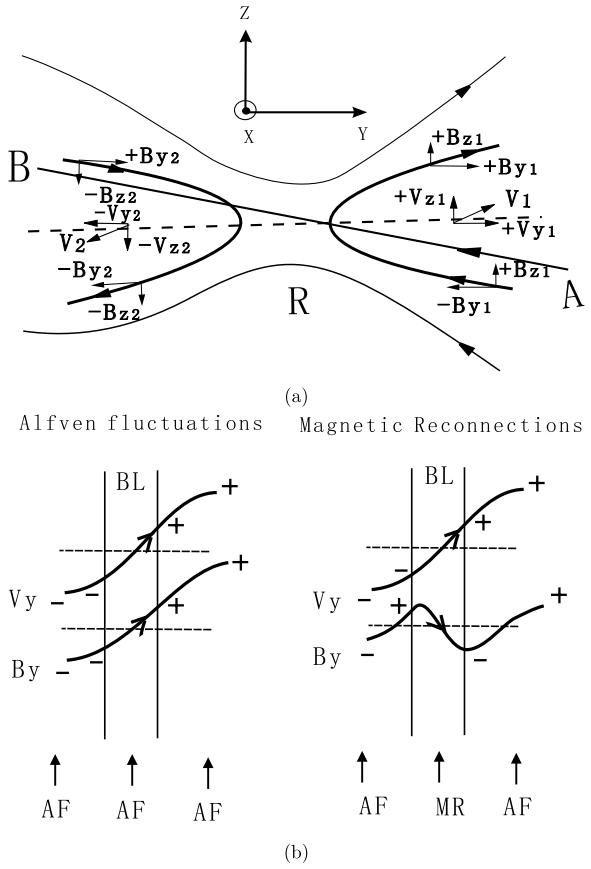

Figure 11. (a) A possible magnetic reconnection "physical picture" in Y-Z plane implied in Figure 9b, where the magnetic reconnection regions R correspond to $D_1 - D_2$ region, and the direct line AB refer to the path of an observer. Here $V_1(V_{y1}, V_{z1})$, B_{y1}, B_{z1} and $V_2(V_{y2}, V_{z2})$,B_{y2}, B_{z2} refer to the parameters of the entrance and outgoing sides for the R region; (b) Sketch of different sign relations in the BL caused by the Alfvenic fluctuation (left) and the magnetic reconnection (right), where the horizontal short lines indicate the x-axis position. The AF and MR denote the sign relation caused by Alfvenic fluctuation and magnetic reconnection process, respectively.

are some important manifestations that could be observed in a magnetic reconnection region. These features have been observed in the BLs, as given in subsection 3.2. Here, the discussion, as an example, is focused on a possible interpretation for the reversal flows and fields in the region, $D_1 - D_2$, in Figure 9b. Figure 11a shows a physical scenario with one magnetic reconnection region, R, in the Y-Z plane, which is a main interaction plane, because the direction of the cloud's motion is mainly in X-direction in the GSE coordinate system. When an observer, along the path AB, passes the region R, the recording signatures will follow $+V_y1 \rightarrow -V_y2$, $-B_y1 \rightarrow +B_y2$, $+V_z1 \rightarrow -V_z2$, $+B_z2 \rightarrow -B_z2$, where numbers 1 and 2 refer to the "entrance side" and the "outgoing side" for the investigated region, R. The expected sign variations in the flows and fields in the R region in (Figure 11a) are the same as the observed sign variations in $D_1 - D_2$ region in Figure 9b. Noticing that these variations in the reversal flows and magnetic fields in Figures 9b–10b are not Alfven-type fluctuations because the sign relations shown between the velocity (V_x, V_y, V_z) and the magnetic field (B_x, B_y, B_z) in the BL do not obey the Alfven relations. First, the identifiable reversal flows and fields occurring in the BLs with the field's dip and abrupt directional variations are not related to other structures shown in the SW and MC. Second, the sign variations in the velocity and field inside the BL, i.e., $+V_y1 \rightarrow -V_y2$, $-B_y1 \rightarrow +B_y2$, $+V_z1 \rightarrow -V_z2$, and $+B_z1 \rightarrow -B_z2$ in Figure 9b are different from the sign relation in the Alfven fluctuations where the signs of the V_x/B_x, V_y/B_y and V_z/B_z must be the same, either "plus" or "minus," to each component x, y, and z, for instance, $+V_y1 \rightarrow -V_y2$, $-B_y1 \rightarrow +B_y2$, $+V_z1 \rightarrow -V_z2$, and $-B_z1 \rightarrow +B_z2$ for the "minus" case. Notice that the sign of the B_z here varies from $-B_z1 \rightarrow +B_z2$ in the fluctuation into $+B_z1 \rightarrow -B_z2$ in the magnetic reconnection. Concerning this point, a simple explanation is given in Figure 11b. When an observer passes through the BL, as sketched in Figure 11b, the same direction variation, $-V_y \rightarrow +V_y$, $-B_y \rightarrow +B_y$, could be observed for Alfven fluctuation because the same sign variation is maintained (the left figure), and the opposite variation, $-V_y \rightarrow +V_y$, $+B_y \rightarrow -B_y$, could be observed for magnetic reconnection because the direction in B_y is changed from $-B_y \rightarrow +B_y$ into $+B_y \rightarrow -B_y$ due to the field reconnection process (the right figure). From the analysis above, we see that this consistency between the observations and reconnection expectance in the reversal flows and fields exists in the BLs investigated. In addition, the observed heating, acceleration, and field's dip in the field reversal region associated with a sudden field direction variation ($\Delta\phi \sim 180°$, $\Delta\theta \sim 90°$) are also in agreement with those expected from the magnetic reconnection region (such as region R in Figure 11a). Up to now, we have seen that these variations in all parameters expected by the magnetic reconnection picture in Figure 11a are qualitatively consistent with the parameter variations observed by Wind across $M_t - G_t$ in Figures 9a–9b. This means that these plasma and field characteristics inside the BLs, as shown in Figures 1–2, could be associated with the magnetic reconnection process within them. Similar structures were observed in the magnetic reconnection regions for the Earth's magnetopause and magnetotail [*Galvin et al.*, 1987; *Rijnbeek et al.*, 1989; *Øieroset et al.*, 2001]. Recently, the accelerated ion flow observed within magnetic field reversal regions in the solar wind was reported as direct evidence for magnetic reconnection in the solar wind near 1 AU by *Gosling et al.* [2005].

[18] Furthermore, in order to enhance our understanding of the nature of the new non-pressure-balanced structures, we now discuss the difference between the JL of shock waves and the BL of MCs. Figure 12a is a typical interplanetary shock wave event beginning at ≈1800 UT on 19 August 1998, which was driven by a MC beginning at ≈0910 UT on 20 August 1998. Where the letters S and M_f, G_f on the top of the figure represent the shocked surface and the cloud's boundary layer, respectively, and all the parameters have their usual meanings. Figures 12b and 12c give some basic parameters in the jump layer, $J_f - L_f$, of the shocked surface and the boundary layer, $M_f - G_f$, respectively. Comparing them shows that they are two different kinds of non-pressure-balanced structures. From Figure 12b we can clearly see that the basic parameters, such as

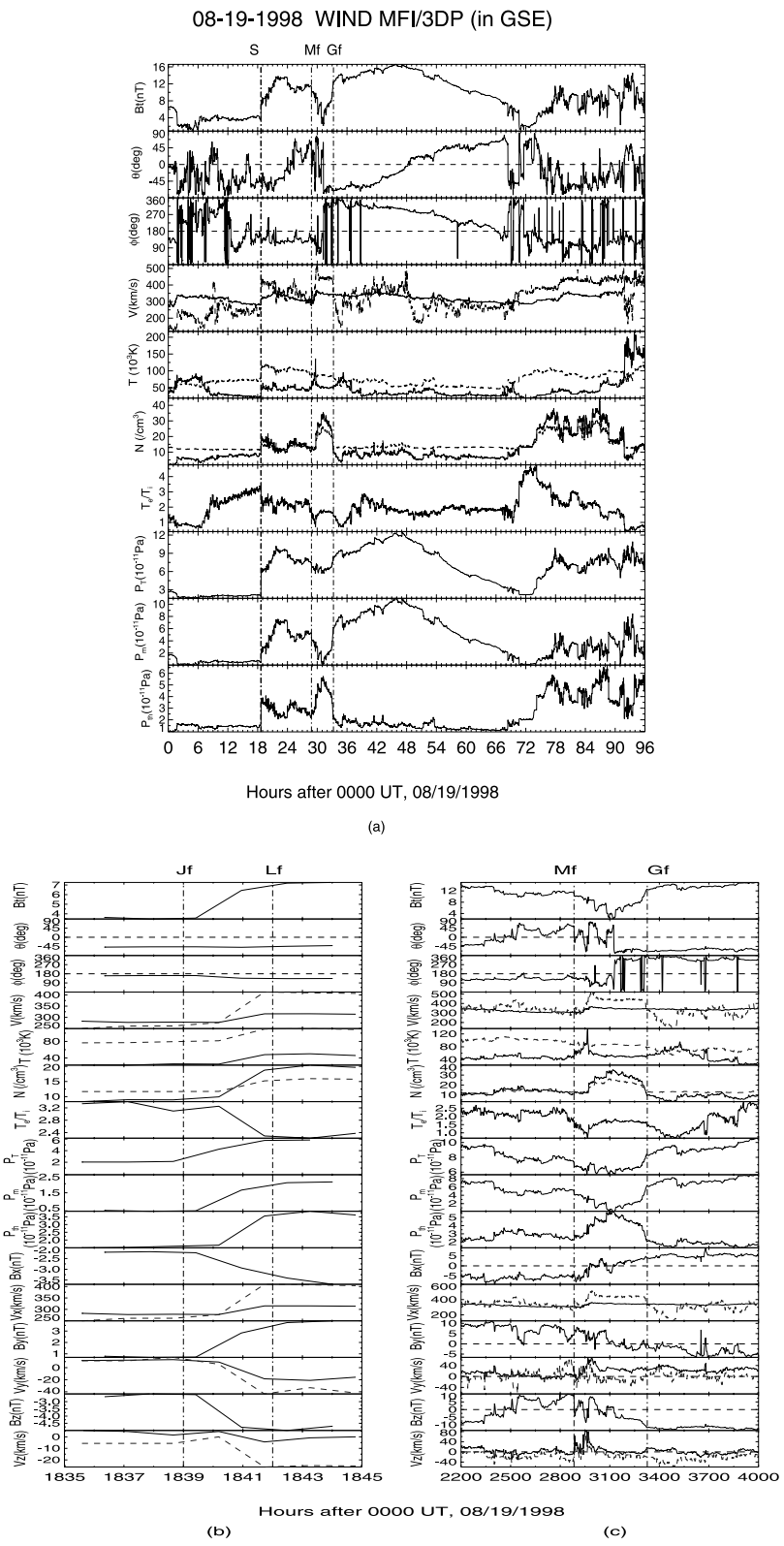

Figure 12. (a) A typical interplanetary shock wave event on August 19, 1998, where "S," M_f and G_f on the top of the figure stand for shocked surface and the BL, (b) the shock wave's jump layer, $J_f - L_f$, and (c) the magnetic cloud's boundary layer, $M_f - G_f$, in the basic parameters B_t, θ, ϕ,V, T, N, T_e/T_i, P_T, P_m, P_{th}, B_x, V_x, B_y,V_y, B_z and V_z, where all parameters have the usual meanings.

magnetic field strength, B_t, velocity, V, temperature, T, number density, N, total pressure, P_T, magnetic pressure, P_m, and thermal pressure, P_{th}, display a rapid increase in the JL and continually keep up a high level in the sheath region, but these variations in the basic parameters for the MC boundary layer, $M_f - G_f$, occur mainly in the BL where the magnetic field strength, B_t, and magnetic pressure, P_m are decreasing. At the same time, the obviously different behavior also appears in other basic parameters. Almost no significant changes appear in the JL, in this particular case, whereas an abrupt, large-amplitude variations, $\Delta\theta \approx 90^\circ$, $\Delta\phi \approx 180^\circ$, and reversal flows ($V_x$, V_y,V_z) and bipolar field profiles (B_x, B_y, B_z) that are seldom observed in the JL, can be frequently seen in the BL. It should be noticed that these characteristics in the JL are very common in many shock wave events. The markedly different properties between the JL and the BL imply different dynamic processes occurring in them. The former, as is well known, is a nonlinear steepening process caused by the supersonic flow with the flow velocity larger than the fast magnetosonic velocity in the local medium, and the latter is possibly associated with the magnetic reconnection process in the BL, as mentioned in the discussion above. The comparisons here tell us that the MC's boundary layer is a new nonpressure-balanced structure possibly associated with the magnetic reconnection process occurring in interplanetary space. This topic attracts our further attention on analyzing plasma wave activity and the accelerated particle flux to further understand the BLs. The related work is under consideration.

[19] Summarizing the results reported and the discussions in this paper, we conclude that the BL of a MC is a new non-pressure-balanced structure with a decreased magnetic pressure for about 90% of the BLs investigated. Heating and acceleration of the protons, electrons, and α particles are also general for about >80% of the BLs, and the events of the reversal flows and fields are also observed in ≈83% of the BLs, far higher statistically than that of the SW and the MC. This shows that the BLs possess the plasma and field characteristics different from those in the SW and MC, as they have their own magnetic structures different from those of SW and MC [*Wei et al.*, 2003a]. The nature of the MC's boundary layer completely differs from that of the shock wave's jump layer, which is determined by their different dynamic processes. These plasma characteristics in the BLs are consistent with the dynamic behavior expected from the magnetic reconnection picture. Therefore we can deduce that as one interpretation, the magnetic reconnection process is possibly occurring in the BLs. The present study for the BL's nature is in an initial status. Many problems such as the plasma wave activity [*Burlaga et al.*, 1980], particle acceleration and their formation mechanism in the BLs, and the effect on the coupling process between the MC and the magnetosphere need further study.

[20] **Acknowledgments.** We appreciate NASA CDAWEB for publishing the Wind solar wind and magnetic field data. We are grateful to the Wind MFI (PI, R. Lepping, GSFC) team for identifying the magnetic clouds observed by the Wind spacecraft. This work is jointly supported by NSFC grant 40336053, 40536029, 40523006, and 40374056. This work was also supported in part by the International Collaboration Research Team Program of the Chinese Academy of Sciences.

[21] Shadia Rifai Habbal thanks Ronald P. Lepping and Katsuhide Marubashi for their assistance in evaluating this paper.

References

Belcher, J. W., and L. Davis Jr. (1971), Large-amplitude Alfven wave in the interplanetary medium, *J. Geophys. Res.*, *76*, 3534–3563.

Bothmer, V., and R. Schwenn (1994), Eruptive prominences as sources of magnetic clouds in the solar wind, *Space Sci. Rev.*, *70*, 215–220.

Burlaga, L. F. (1968), Micro-scale structures in the interplanetary medium, *Solar Phys.*, *4*, 67–92.

Burlaga, L. F. (1971), Hydrodynamic waves and discontinuities in the solar wind, *Space Sci. Rev.*, *12*, 600–657.

Burlaga, L. F. (1995), *Interplanetary Magnetohydrodynamics*, pp. 45–69, Oxford Univ. Press, New York.

Burlaga, L. F., et al. (1980), Interplanetary particles and fields, November 22 to December 6, 1977: Helios, Voyager and IMP observations between 0.6 AU and 1.6 AU, *J. Geophys. Res.*, *85*, 2227–2242.

Burlaga, L. F., S. F. Mariani, and R. Schwenn (1981), Magnetic loop behind an interplanetary shock: Voyager, Helios and IMP8 observations, *J. Geophys. Res.*, *86*, 6673–6684.

Burlaga, L. F., J. D. Scudder, L. W. Klein, and P. A. Isenberg (1990), Pressure balanced structures between 1 AU and 24 AU and their implications for solar wind electrons and interstellar pick up ions, *J. Geophys. Res.*, *95*, 2229–2239.

Farrugia, C. J., R. J. Fitzenreiter, L. F. Burlaga, N. V. Erkaev, V. A. Osherovich, H. K. Biernat, and A. Fazakerley (1994), Observations in the sheath region ahead of magnetic clouds and in the dayside magnetosheath during cloud passage, *Adv. Space Res.*, *14*(7), 105–110.

Farrugia, C. J., L. F. Burlaga, and L. P. Lepping (1997), Magnetic clouds and the quiet-storm effect at earth, in *Magnetic Storms*, *Geophys. Monogr. Ser.*, vol. 98, edited by B. T. Tsurutani et al., pp. 91–106, AGU, Washington, D. C.

Farrugia, C. J., et al. (2001), A reconnection layer associated with a magnetic cloud, *Adv. Space Res.*, *28*(5), 759–764.

Fitzenreiter, R. J., and L. F. Burlaga (1978), Structure of current sheets in magnetic lates at 1 AU, *J. Geophys. Res.*, *83*, 5579–5585.

Galvin, A. B., F. M. Ipavich, G. Gloeckler, D. Hovestadt, S. J. Bame, B. Klecker, M. Scholer, and B. T. Tsurutani (1987), solar wind iron charge states preceding a driver plasma, *J. Geophys. Res.*, *92*, 12,069–12,081.

Gosling, J. T., D. N. Baker, S. J. Bame, W. C. Feldman, and R. Zwickl (1987), Bidirectional solar wind electron heat flux events, *J. Geophys. Res.*, *92*, 8519–8535.

Gosling, J. T., R. M. Skoug, D. J. McComas, and C. W. Smith (2005), Direct evidence for magnetic reconnection in the solar wind near 1 AU, *J. Geophys. Res.*, *110*, A01107, doi:10.1029/2004JA010809.

Innes, D. E., B. Inhester, W. I. Axford, and K. Wilhelm (1997), Bi-directional plasma jets produced by magnetic reconnection on the Sun, *Nature*, *386*, 811–813.

Lepping, R. P., et al. (1997), The Wind magnetic cloud and events of October 18–20, 1995: Interplanetary properties and as triggers for geomagnetic activity, *J. Geophys. Res.*, *102*, 14,049–14,063.

Marsch, E., K. H. Muhlhauser, H. Rosenbauer, R. Schwenn, and F. M. Neubauer (1982), Solar wind Heliom Ions: Observations of the Helios solar probes between 0.3 and 1AU, *J. Geophys. Res.*, *87*, 35–51.

Øieroset, M., T. D. Phan, M. Fujimoto, R. P. Lin, and R. P. Lepping (2001), In situ detection of collisonless reconnection in the earth's magnetecotail, *Nature*, *412*, 414–417.

Osherovich, V., and L. F. Burlaga (1997), Magnetic clouds, in *Coronal Mass Ejections*, *Geophys. Monogr. Ser.*, vol. 99, edited by N. Crooker, J. A. Joselyn, and J. Feynman, pp. 157–168, AGU, Washington, D. C.

Paschmann, G., B. U. Ö Sonnerup, and I. Papamastorakis (1979), Plasma acceleration at the Earth's magnetopause: Evidence for reconnection, *Nature*, *282*, 243–246.

Rijnbeek, R. P., H. K. Biernat, M. F. Heyn, V. S. Semenov, C. J. Farrngia, D. J. Southwood, G. Paschmann, N. Sckopke, and C. T. Russel (1989), The structure of the reconnection layer observed by ISEE 1 on 8 September 1978, *Ann. Geophys.*, *7*, 297–310.

Steinberg, J. T., A. J. Lazarus, K. W. Ogilvie, R. Lepping, and J. Byrnes (1996), Differential flow between solar wind protons and alpha particles: First Wind observations, *Geophys. Res. Lett.*, *23*, 1183–1186.

Tsurutani, B. T., and W. D. Gonzalez (1997), The interplanetary causes of magnetic storms: A review, in *Magnetic Storms*, *Geophysical Monogr. Ser.*, vol. 98, edited by B. T. Tsurutani et al., pp. 77–89, AGU, Washington, D. C.

Tsurutani, B. T., W. D. Gonzalez, F. Tang, S. I. Akasofu, and E. J. Smith (1988), Origin of interplanetary sourthward magnetic fields responsible for major magnetic storms near solar maximum (1978–1979), *J. Geophys. Res.*, *93*, 8519–8531.

Tsurutani, B. T., et al. (1998), The January 10, 1997 auroral hot spot, horseshoe aurora and first substorm: A CME loop?, *Geophys. Res. Lett.*, *25*, 3047–3050.

Turner, J. M., L. F. Burlaga, N. F. Ness, and J. F. Lemaire (1977), Magnetic holes in the solar wind, *J. Geophys. Res.*, *82*, 1921–1924.

Wei, F. S., R. Liu, X. Feng, D. Zhong, and F. Yang (2003a), Magnetic structures inside boundary layers of magnetic clouds, *Geophys. Res. Lett.*, *30*(24), 2283, doi:10.1029/2003GL018116.

Wei, F. S., R. Liu, Q. Fan, and X. Feng (2003b), Identification of the magnetic cloud boundary layers, *J. Geophys. Res.*, *108*(A6), 1263, doi:10.1029/2002JA009511.

Winterhalter, D., M. Neugebauer, B. E. Goldstein, E. J. Smith, S. J. Bame, and A. Balogh (1994), Ulysses field and plasma observations of magnetic holds in the solar wind and their relation to mirror-mode structure, *J. Geophys. Res.*, *99*, 23,371–23,381.

Zwickl, R. D., J. R. Asbridge, S. J. Bame, W. C. Feldman, J. T. Gosling, and E. J. Smith (1983), Plasma properties of driver gas following interplanetary shocks observed by ISEE-3, in *Solar Wind Five*, edited by M. Neugebauer, *NASA Conf. Publ.*, *CP-2280*, 711.

X. Feng, F. Wei, F. Yang, and D. Zhong, SIGMA Weather Group, Key Laboratory for Space Weather, Center for Space Science and Applied Research, Chinese Academy of Sciences, P. O. Box 8701, Beijing, 100080, China. (fengx@spaceweather.ac.cn)